JCTC Journal of Chemical Theory and Computation

Article

pubs.acs.org/JCTC

Efficient Two-Step Procedures for Locating Transition States of Surface Reactions

Astrid Nikodem,[†] Alexei V. Matveev,[†] Bo-Xiao Zheng,[†,‡] and Notker Rösch*[,†,§]

[†]Department Chemie and Catalysis Research Center, Technische Universität München, 85747 Garching, Germany

[‡]Department of Chemistry and Key Laboratory of Organic Optoelectronics and Molecular Engineering of Ministry of Education, Tsinghua University, Beijing 100084, China

[§]Institute of High Performance Computing, 1 Fusionopolis Way, #16-16 Connexis, Singapore 138632, Singapore

Supporting Information

ABSTRACT: Using various two-step strategies, we examined how to accurately locate transition states (TS) of reactions using the example of eight reactions at metal surfaces with 14–33 moving atoms. These procedures combined four path-finding methods for locating approximate TS structures (nudged elastic band, standard string, climbing image string, and searching string, using a conjugate gradient or a modified steepest-descent method for optimization and two types of coordinate systems) with subsequent local refinement by two dimer methods. The dimer-Lanczos variant designed for this study required on average 20% fewer gradient calls than the standard dimer method. During the path finding phase, using mixed instead of Cartesian coordinates reduced the numbers of gradient calls on average by an additional 21%, while using a modified steepest-descent method improved that key efficiency criterion on average by 13%. For problematic cases we suggest strategies especially adapted to the problem at hand.

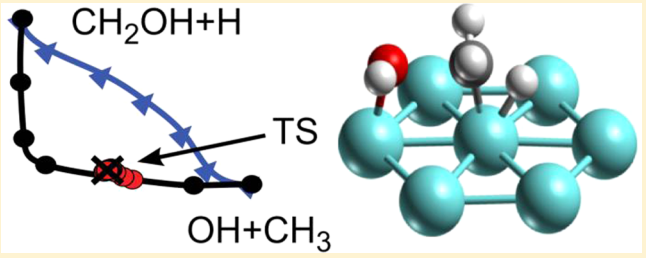

1. INTRODUCTION

For elucidating the mechanism of a complex chemical reaction and the corresponding rates, it is essential to determine structures and energies of transition states (TSs). The latter are commonly estimated by approximating the corresponding first-order saddle points on a potential energy surface. TSs are notably more difficult to locate than local minima, which probably explains why a variety of specialized methods have been suggested.[1−4] One type of strategy for finding TSs uses the highest-energy point on a minimum energy path that connects two local minima.[2] Alternatively, so-called local searching methods refine the guess of a starting structure; these methods are unable to guarantee that reaction pathways starting from a located stationary point reach the intended local minima.[3,5,6] For the targets of this study, reactions on solid surfaces, both types of methods are well established. Although they usually are used separately, we will combine one method of each type into a two-step strategy, to facilitate and, to some extent, automatize the accurate determination of TSs.

If one needs only a rough estimate of a TS, chain-of-states methods can be useful for constructing a point-wise approximation of a reaction path. Among these procedures, the nudged elastic band method (NEB)[7,8] is most prominently used for reactions at surfaces.[9−11] In the NEB method, "spring" forces are invoked to achieve a uniform distribution of the states (images) along the approximate minimum energy path. Alternative string methods[12,13] attempt to decouple the problem of finding a discrete representation of a minimum energy path from the problem of choosing an appropriate distribution of the selected points. Although well studied,[13−19] these alternative methods are rarely applied to surface reactions.[20] Part of that research aims at improving the TS estimate derived from a given path. An obvious solution is to increase the density of images close to the anticipated location of the TS.[21] One such strategy parametrizes the reaction path using an energy-weighted arc length.[22] Another approach invokes an improved electronic structure quantum method for a substring.[18] In our previous work,[14] we suggested adding new images near the expected TS.

When an accurate structure of a TS is required, these path methods are in general not sufficient because they solve the subtly different problem of approximating a path rather than locating a TS. The climbing image (CI) approach, a modification of the NEB or string methods, is a notable exception as it does not treat all images on an equal footing.[21,22] Rather, the image with highest energy is supposed to climb to the TS. This made the CI variant of the NEB method recently very popular for treating surface reactions.[23−31]

Local TS search methods, like the dimer method,[32−34] require a good initial guess, but even then there is no guarantee that the TS located lies on the intended path. Yet, the dimer method is also popular for exploring surface reactions.[35,36] In view of the advantages and disadvantages of the two types of

Received: August 20, 2012

   dx.doi.org/10.1021/ct300728a | J. Chem. Theory Comput. XXXX, XXX, XXX−XXX

procedures, it appears reasonable to invoke a two-step strategy where a TS estimate from a path optimization method is subsequently refined by a local method. This combination strategy has already been used for CI-NEB and dimer methods.[37,38] Also in our group, NEB and dimer approaches have been applied in combination.[39−42]

Systematic studies of methods for locating transition states used simple analytical potentials[2,43,44] or worked with *ab initio* potentials on gas phase reactions[3,14] or with a mixture of both kinds of potentials.[16] As examples of TS search for surface reactions, we mention the work of Sheppard et al., who modeled surface diffusion of Pd_4 clusters on MgO(100) as well as dissociative adsorption of molecular oxygen and diffusion of atomic oxygen on Au(111),[45] using the CI-NEB and the CI-string methods combined with various path optimization procedures; the results obtained depended more on the optimization process than on the chain-of-states method. Klimeš et al. analyzed the performance of the dimer method for diffusion of water and the dissociative adsorption of HCl on a NaCl surface,[46] concluding that the performance of the dimer method varies notably from one system to the other.

The present study focuses on reactions at metal surfaces where bonds in adsorbates are formed and broken. For such catalytically relevant problems, a systematic evaluation of two-step approaches, probing various method combinations, is still lacking. The test set examined comprised eight surface reactions involving the breaking or formation of C−H, C−C, C−O, and O−H bonds for adsorbates of 5−24 atoms. The reactants were larger, hence closer to surface reactions of current interest, than those used earlier in a similar study.[46]

For the present work, we extended an existing collection of utilities[14,47] by local refinement methods and systematically explored two-step strategies by combining various path searching and local refinement methods. Among the path searching methods, we included a CI-string variant which in principle could search on its own for a TS, but we looked for a more efficient approach by terminating the CI optimization early, to be followed by a presumably less expensive local TS search. The CI method may require more gradient evaluations than a local refinement method (e.g., dimer method) because the accuracy of the TS estimate is only increasing as fast as the overall accuracy of the discrete path.

This paper is structured as follows. Section 2 introduces the methods. Section 3 presents the test systems and computational details. In section 4, we systematically compare the performance of method combinations on a subset of four test systems, addressing in turn path-searching methods, local refinement methods, and their various combinations. We also probe the performance of the best combinations determined on the remaining four test systems. Finally, in section 5, we offer some conclusions.

2. CHAIN-OF-STATES AND DIMER METHODS

2.1. Chain-of-States Methods. As most search methods applied here have been described elsewhere,[8,12,14,22,45] we restrict the following discussion to details specific to the present work. Our implementation of the NEB method follows that of Henkelman and Jónsson.[8] The standard versions of the string method and the searching-string method are essentially those of our previous work,[14] except that the spline interpolations of third order for each component x^j of the vector-valued path parametrization $\mathbf{x}(s)$ here are built with the constraint that differences $s_{i+1} - s_i$ are proportional to $|\mathbf{x}_{i+1} - \mathbf{x}_i|$. Images are redistributed using the lengths of the path segments obtained by numerically integrating the slope $|d\mathbf{x}/ds|$. This "re-spacing"' is only applied if any path segment deviates in length from its target value by more than a threshold. We also implemented a CI-string method following Weinan et al.[22] The images of the two substrings between the minima and the climbing image are respaced separately using the same strategy as for the standard string method.

We optimize the paths using two strategies: (*i*) a conjugate-gradient method operating on the geometry of the whole chain and (*ii*) a set of optimizer instances applying an optimized variant of the steepest-descent method for every chain image.[14] We refer to the latter variant as "multiopt". As the tangent is a function of the chain geometry, multiopt instances are not completely independent.

The conjugate-gradient method implemented resembles a previously published variant.[45] The search direction $\mathbf{Q}^{(n)} = [\mathbf{q}_1^{(n)} ... \mathbf{q}_N^{(n)}]$ for step n is calculated using the Polak−Ribiere formula[48] for conjugate gradients, $\mathbf{Q}^{(n)} = \mathbf{F}^{(n)} + \gamma^{(n)}\mathbf{Q}^{(n-1)}$, with the restriction $\gamma^{(n)} = \max[\mathbf{F}^{(n)T}(\mathbf{F}^{(n)} - \mathbf{F}^{(n-1)})/|\mathbf{F}^{(n-1)}|^2, 0]$.[48] $\mathbf{F}^{(n)} = [\mathbf{f}_1^{(n)} ... \mathbf{f}_N^{(n)}]$ is the vector of modified forces on the images. We found it convenient to carry out a single Newton step along the search direction $\mathbf{Q}^{(n)}$ where the slope was approximated as the finite difference of the projection $\mathbf{F}^T\mathbf{Q}^{(n)}$ of the modified forces $\mathbf{F}$.[45] An accurate line search when seeking the root of the force projection $\mathbf{F}^T\mathbf{Q}^{(n)}$ does not seem to be reasonable, in part due to the interaction with the redistribution of images. A backtracking step is carried out when the projection of the force changes sign but does not decrease by absolute value. The step length is restricted by a user-defined value.

The multiopt optimizer defines the search direction $\mathbf{q}_i^{(n)}$ for image i as the steepest-decent direction, $\mathbf{q}_i^{(n)} = \mathbf{f}_i^{(n)}$.[14] An approximate representation of the Hessian is maintained with an SR1 update;[48] together with the energy gradient, it provides a quadratic approximation of the potential energy surface. This quadratic model is used to estimate the location of the energy minimum in the steepest-descent direction. A trust radius limits the magnitude of the changes, of the overall geometry and the various images.[14] As for the conjugate-gradient method, a redistribution of string images may follow. The multiopt procedure was designed only for use in combination with string methods, not with NEB.

2.2. Dimer Methods. *2.2.1. The Standard Dimer Method.* The standard dimer method keeps the updated geometry $\mathbf{x}_c$ of the assumed midpoint of the dimer, approximating the TS, and the mode vector $\mathbf{m}$ that approximates the direction of the lowest curvature on the potential energy surface. Shifting the location $\mathbf{x}_c$ (translation) alternates with updating the direction $\mathbf{m}$ (rotation).[33] Our variant follows in general earlier implementations.[33,49]

The rotation plane is defined by the current mode vector $\mathbf{m}^{(n)}$ and an orthogonal vector $\mathbf{k}^{(n)}$ derived from the difference $\Delta\mathbf{g}(\mathbf{m}^{(n)})$ of gradients at position $\mathbf{x}_c$ and a position in the direction of $\mathbf{m}^{(n)}$. A special version of the Polak−Ribiere formula[48] for the recurrence relation $\mathbf{k}^{(n)} \rightarrow \mathbf{m}^{(n+1)}$ yields the conjugate rotation axes of successive iterations.[32]

The curvatures of the potential energy surface along a direction $\mathbf{p}$ in the rotation plane is given by a function $C(\psi)$ of angle $\psi = \angle(\mathbf{m},\mathbf{p})$. Assuming a quadratic form of the potential energy surface, the three coefficients of a harmonic expansion of the curvature $C(\psi)$ are obtained by fitting C and its derivative $dC/d\psi$ at $\psi = 0$ and at a second angle, say $\psi = 45°$.[33]

dx.doi.org/10.1021/ct300728a | J. Chem. Theory Comput. XXXX, XXX, XXX−XXX

The minimum ψ_0 of $C(\psi)$ defines the new mode direction.[33] Rotations are terminated when either (*i*) a given maximum number of iterations has been reached, or (*ii*) a preliminary estimate $\tilde{\psi}_0$ of the rotation angle is below a given threshold, or (*iii*) the computed location of the minimum ψ_0 is below that threshold.[33]

For the translation of the midpoint $\mathbf{x}_c$, a modified force, $\mathbf{f}_c = -\mathbf{g}_c + 2\mathbf{g}_c^{\parallel}$, with the gradient component $\mathbf{g}_c^{\parallel}$ along direction $\mathbf{m}$ being inverted, is applied to generate a conjugate-gradient search direction along which a Newton step is carried out. To estimate the energy profile along the search direction, an additional trial step is made initially.[32] The step length is reduced if it exceeds a user-defined threshold. For a positive curvature *C*, the dimer is moved instead by a maximum step length in the direction $(\mathbf{m}^T\mathbf{g}_c)\mathbf{m}$.[32]

2.2.2. The Modified Dimer-Lanczos Method. We implemented a further method, referred to as modified dimer-Lanczos (mDL) method, for local TS searches in the spirit of the dimer method, but we employed a Lanczos procedure for mode updating.[44] As a novel aspect of the present implementation, we combined information on the lowest-frequency mode from the Lanczos iterations and the approximate Hessian for the midpoint updating. Similar to Shang and Liu,[5] who used the dimer method together with a constrained Broyden minimization,[6] we combined the method for generating an approximate eigenmode and a quasi-Newton translation algorithm.

In more detail, for the mode update, we iteratively build an orthonormal basis $\{\mathbf{b}^{(n)}\}$ starting from the mode vector $\mathbf{b}^{(0)} = \mathbf{m}^{(0)}$. One constructs a new basis vector $\mathbf{b}^{(n+1)}$ from the difference $\Delta\mathbf{g}(\mathbf{b}^{(n)})$ of the gradients (section 2.2.1):

$$\mathbf{b}^{(n+1)'} = [1 - \sum_{k<n} \mathbf{b}^{(k)}\mathbf{b}^{(k)T}]\Delta\mathbf{g}(\mathbf{b}^{(n)})$$

$$\mathbf{b}^{(n+1)} = \mathbf{b}^{(n+1)'}/|\mathbf{b}^{(n+1)'}|$$

Within the subspace spanned by $\{\mathbf{b}^{(n)}\}$, one builds an approximation $\mathbf{B}^{(n)}$ to the Hessian:

$$B_{ik}^{(n)} = [\mathbf{b}^{(i)T}\Delta\mathbf{g}(\mathbf{b}^{(k)}) + \mathbf{b}^{(k)T}\Delta\mathbf{g}(\mathbf{b}^{(i)})]/2l_d, \quad i, k < n$$

Matrix $\mathbf{B}^{(n)}$ is symmetric by construction and tridiagonal. In practice, the number of Lanczos iterations is much smaller than the dimension of the coordinate space, notably limiting the space under consideration. The eigenvector for the smallest eigenvalue $C^{(n)}$ of $\mathbf{B}^{(n)}$ is taken as new mode vector $\mathbf{m}^{(n)}$. The Lanczos iterations are repeated until one of the following criteria is fulfilled: (*i*) the angle between mode vectors $\mathbf{m}^{(n)}$ and $\mathbf{m}^{(n-1)}$ is below a threshold, (*ii*) the angle between the mode vector $\mathbf{m}^{(n)}$ and the difference $\Delta\tilde{g}(\mathbf{m}^{(n)})$ of gradients, extrapolated from the results of the basis vectors, is below the same threshold, or (*iii*) the number of iterations reached a preset maximum. Angles were chosen as convergence criteria to allow a more direct comparison with the dimer method, section 2.2.1.

For the update of the midpoint $\mathbf{x}_c$, we combine the strength of a quasi-Newton approach in searching for stationary points with the advantages of the dimer method. As appropriate for a local TS search, it is ensured that the structure of the inverse Hessian $\mathbf{H}$ has exactly one mode with negative eigenvalue near the TS. To this end, the approximate inverse Hessian $\mathbf{H} = \mathbf{H}_+ + \Delta\mathbf{H}$ is created from two contributions, a positive definite inverse Hessian $\mathbf{H}_+$ maintained by BFGS updates[48] and the contribution $\Delta\mathbf{H}$ for the eigenvalue C^{-1} in the mode direction $\mathbf{m}$ provided by the Lanczos method.

The BFGS updates are carried out with gradients and steps calculated in the Lanczos iterations followed by an update with the gradients and steps of the dimer midpoint. Thus, at variance with the conventional dimer method, our approach uses more information from the mode update than only the mode direction $\mathbf{m}$ and the sign of the approximate eigenvalue *C*. The second part of the inverse Hessian $\mathbf{H}$ is the symmetric rank−1 contribution $\Delta\mathbf{H} = \mathbf{u}\mathbf{u}^T/(\mathbf{u}^T\mathbf{y})$ where $\mathbf{u} = \mathbf{m} - \mathbf{H}_+\mathbf{y}$ is derived from the mode direction $\mathbf{m}$ and $\mathbf{y} = C\mathbf{m}$, resembling a gradient difference in mode direction. As a consequence, the inverse Hessian features the eigenmode $\mathbf{m}$ with eigenvalue C^{-1}, which is negative in the nonconvex regions. The updated inverse of the Hessian is used to calculate the quasi-Newton translation $\Delta\mathbf{x}_c = -\mathbf{H}\mathbf{g}_c$ of the midpoint. This strategy is to be compared with the conjugate-gradient approach of the conventional dimer method, section 2.2.1, that requires an additional gradient calculation for approximating the energy profile along the search direction.

As in the standard dimer method, the step length is restricted also in the mDL approach. For a positive value of *C*, the step is exchanged by a full minimizing step in the direction perpendicular to mode $\mathbf{m}$, followed by a step in the direction $(\mathbf{m}^T\mathbf{g}_c)\mathbf{m}$, such that the maximum step length is reached.

3. SURFACE REACTION MODELS

3.1. Computational Details. The methods for locating transition structures, as described in section 2, were implemented in the utility package ParaTools,[47] which builds on the Atomic Simulation Environment for interfacing to various quantum chemistry codes.[2,50] The electronic structure calculations were carried out with the Vienna *ab initio* simulation package VASP 4.6,[51,52] applying a plane-wave based density functional approach at the gradient-corrected level.[53] The effect of core electrons was described with the PAW method.[54,55] For benchmarking, we applied an energy cutoff of 320 eV.

We used two sets of coordinates to parametrize potential energy surfaces. Besides Cartesian coordinates (CART), we also employed mixed coordinate systems (MIX) where the metal substrate was described by Cartesian coordinates while internal coordinates were used for the adsorption complexes (Z-matrix). The positions of the adsorbates relative to the metal surface were parametrized by vectors; the rotational orientations of the adsorbates was tracked with the help of quaternions.[56] To interpret properly the tolerance parameters, we note that in ParaTools, lengths are measured in Ångstroms, angles in radians, energies in electronvolts, and gradient components in electronvolts per Ångstrom or electronvolts per radian, respectively.

For the path searching methods, two parameters, Δg and Δx, were compared with preselected convergence thresholds. The measure Δg of gradient convergence is defined as the root-mean-square of the gradient component orthogonal to the path of the moving images; for the climbing image in the CI-string method, the complete gradient was used for generating the root-mean-square Δg. The measure Δx of geometry convergence is defined as the maximum step length for the three images of highest energies during the last three iterations. A path optimization was considered converged if $\Delta g < 0.1$ or $\Delta g < 0.5$ and $\Delta x < 0.03$. In the searching string method, a new image is added when $\Delta g < 0.5$. We allowed at most 35

dx.doi.org/10.1021/ct300728a | J. Chem. Theory Comput. XXXX, XXX, XXX−XXX

iterations of the path optimizer. When the maximum number of images is reached, the chain of the searching string method has seven images (including the two fixed terminal ones). For the other methods, we also used seven images. The climbing image of the CI-string method was started after at most five standard string iterations with the convergence criteria of $\Delta g < 0.5$;[21,22] these iterations were also counted for the statistics.

In the CI-string method the image of highest energy was used to start the dimer methods. For the NEB and the other string methods, an estimate of the TS was extracted with the "spline and polynomial" approach.[14] As a first approximation for the mode vector of the dimer method, we used the tangent of the path. The dimer method was considered converged when the maximum absolute component of the gradient at the midpoint was below 0.02. We admitted at most 150 dimer translations. The dimer methods were always applied in the coordinate system that had been used for the preceding path determination.

Upon convergence of the dimer method, we carried out a normal-mode analysis to confirm the approximate TS as a first-order saddle point. The overall TS search for a system and a method combination was considered successful when this analysis revealed one imaginary vibrational frequency.

3.2. The Test Systems. For the method evaluation, we selected eight model systems inspired by recent investigations of reactions on Pt(111);[39,41,42] see Table 1 and Figure 1. In the present study, we simplified some of the adsorbed species, e.g., by replacing alkyl groups not taking part in the reactions with hydrogen atoms. For computational economy, slab models of Pt(111) with three layers were chosen to describe the metal substrate. We used (3 × 3) surface unit cells and a spacing of at least 10 Å between two slabs. Two metal layers were kept fixed; only the nine atoms (per surface unit cell) of the uppermost layer were allowed to relax together with the adsorbates. The geometries of local minima, reactants, and products, together with reference transition states, were obtained by conventional means. The resulting barrier heights are also given in Table 1.

Table 1. Reactions on Pt(111) Used to Evaluate Combinations of Transition State Search Methods[a]

		reaction	N	ΔE_1	ΔE_2	ref
I	C−H bond formation	$CH_2C + H \rightarrow CH_2CH$	14	55	69	41
II	H-shift	$CH_2CH \rightarrow CH_3C$	14	169	218	41
III	C−C bond breaking	$CH_2CO \rightarrow CH_2 + CO$	14	106	141	57
IV	O−H bond breaking	$CH_3OH \rightarrow CH_3O + H$	15	57	15	39
V	C−H bond breaking	$CH_3OH \rightarrow CH_2OH + H$	15	30	90	39
VI	ring-opening	$\overline{CH_2\ CH_2\ CH_2\ CC\ CH_3}$	24	118	191	42
VII	C−O scission	$CH_2OH + H \rightarrow CH_3 + OH$	15	196	151	58
VIII	OH substitution	$CH_3OH + H \rightarrow CH_4 + OH$	16	221	191	58

[a]Shown are the numbers N of atoms moving during the transition state search, the barriers ΔE_1 and ΔE_2 (kJ/mol) from the reactant and product sides, respectively, to the reference transition structure, obtained by conventional means, as well as references to recent computational studies of related reactions.

A systematic evaluation of methods and method combinations was carried out for the surface reactions I to IV. Two of these models were inspired by recent investigations on transformations of ethylene.[40,41] System I models the formation of a carbon−hydrogen bond: $CH_2C + H \rightarrow CH_2CH$. System II describes a hydrogen shift reaction: $CH_2CH \rightarrow CH_3C$. The other two systems address the breaking of the C−C bond of a ketene, $CH_2CO \rightarrow CH_2 + CO$ (system III),[57] and the scission of the O−H of methanol, $CH_3OH \rightarrow CH_3O + H$ (system IV).[39]

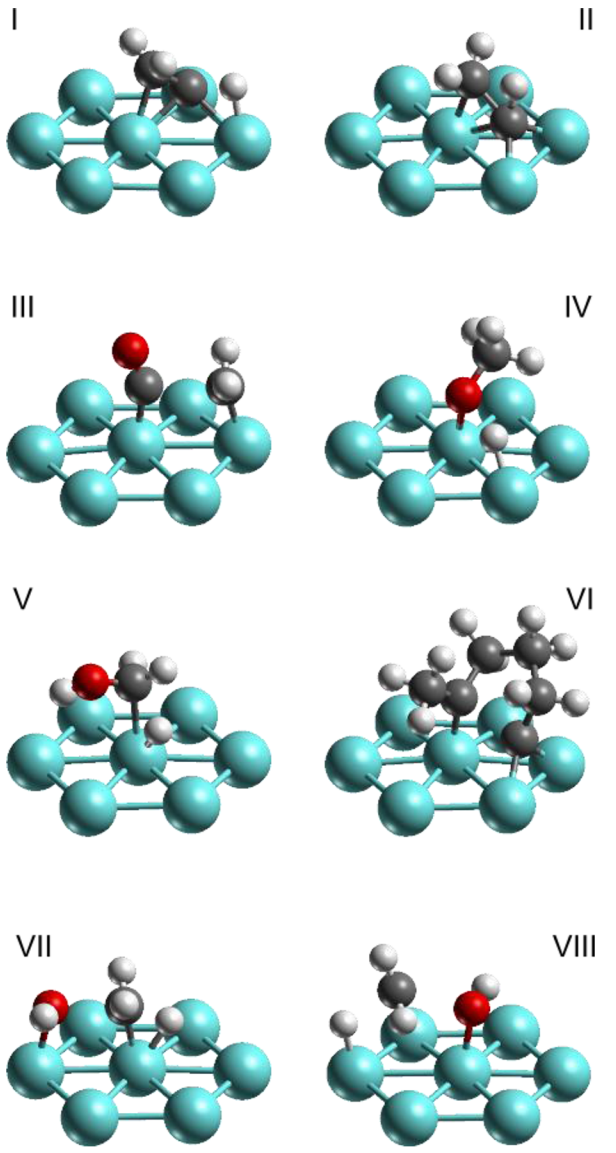

Figure 1. Sketches of the transition states of the various model reactions; see descriptions in Table 1.

The study was extended by examining the four remaining surface reactions, V−VIII, with the two best method combinations and the superior coordinate choice as established by a systematic analysis of the results for systems I−IV. These reactions include breaking a methyl C−H bond of methanol, $CH_3OH \rightarrow CH_2OH + H$ (system V)[39] and ring-opening of cyclopentyne, a simplified $\alpha\alpha\beta\beta$-tetra-adsorbed species that models intermediates in the ring-opening of methylcyclopentane (system VI).[42] With N = 33 moving atoms, the ring-opening model system is the largest one studied in the present work. The remaining two systems model S_N2 reactions. In reaction VII, a C−H bond is formed while a C−O bond is

dx.doi.org/10.1021/ct300728a | J. Chem. Theory Comput. XXXX, XXX, XXX−XXX

broken in concerted fashion, $CH_2OH + H \rightarrow CH_3 + OH$. In reaction VIII, methanol transforms to methane in one step, $CH_3OH + H \rightarrow CH_4 + OH$.

4. RESULTS AND DISCUSSION

4.1. Evaluation of the Path Optimization Step. For each of the systems I–IV, we evaluated all method combinations given in Table 2, applying two choices of coordinate systems. Table 3 reports the resulting number of gradient calls as an efficiency criterion. The three omissions in the table correspond to "failed" path searches where either an atom of the reactants moved into the metal substrate for a significant part of the path or the molecule disintegrated in an undesired fashion. Four path optimizations did not meet the convergence criteria in 35 iterations; see the markers in Table 3. In the last iteration of the three cases involving system I, the gradient convergence measure Δg (section 3.1) was 0.35 and 0.41 for the searching string methods and 0.12 when applying the string method. Likewise, the calculation stopped at Δg = 0.69 in the nonconverged string run of system II. We do not consider these calculations as failures as they do provide an initial guess of a TS for subsequent local optimization. Note that conjugate gradient optimization requires two gradient calls per moving image in every iteration and that the searching string method operates with fewer moving images than the other methods, thus having an advantage in case of a nonconverging path.

Table 2. Path Searching Strategies As Combinations of Four Chain-of-State Methods and Two Path Optimization Procedures, Conjugate Gradient and "multiopt" (See Text)

	optimizer	
chain-of-state method	conj. grad. (CG)	multiopt (MUL)
nudged elastic band (NEB)	yes	no
standard string (S)	yes	yes
searching string (SS)	yes	yes
climbing-image string (CIS)	yes	yes

Figure 2 compares the relative performance of various method categories, such as coordinate systems or optimizer variants etc. For this purpose, we first calculated for a given method and a given system s the relative deviations $\Delta n/\overline{n}_s = (n - \overline{n}_s)/\overline{n}_s$ of the number of gradient calls n from the number $\overline{n}_s$ of gradient evaluations averaged over all methods. This criterion of relative differences reduces the dependence of the performance measure on the overall complexity of a system. To distinguish the performance of method categories, we form the averages $\langle \Delta n/\overline{n}_s \rangle$ of the relative difference over all optimizations falling into these categories. In the latter case, we did not include failed calculations so that the relative performance measure is still somewhat biased.

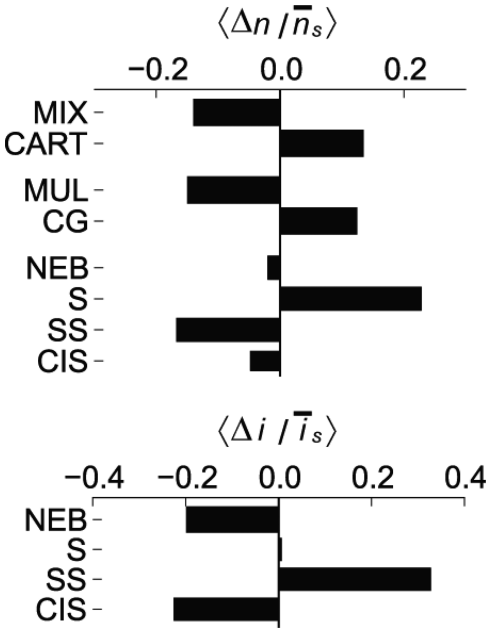

Figure 2. Comparison of the computational efficiency based on average relative differences $\langle \Delta n/\overline{n}_s \rangle$ where $\Delta n = n - \overline{n}_s$ is the difference of the number n of gradient evaluations for systems s = I–IV and the corresponding average $\overline{n}_s$. Lower is better. Compared are mixed (MIX) and Cartesian (CART) coordinates; two optimization procedures, multiopt (MUL) and conjugate gradient (CG); and four chain-of-state methods, NEB, standard string (S), searching string (SS), and CI-string (CIS). Analogous category averages $\langle \Delta i/\overline{i}_s \rangle$ of the relative differences of the number i of chain instances to be calculated from the system-specific average $\overline{i}_s$ for the four chain-of-state methods.

On average, optimizations required fewer gradient calls when carried out with mixed rather than Cartesian coordinates. In 18 cases, mixed coordinates were better, while in only seven cases were the Cartesian more efficient. This is quantified by the relative performance measure $\langle \Delta n/\overline{n}_s \rangle$, which is −0.14 for mixed and 0.13 for Cartesian coordinates (Figure 2). In other words, the former strategy requires on average ∼25% fewer gradient calls than the latter.

Table 3. Number of Gradient Evaluations for Various Chain-of-State Methods[a] in Combination with a Path Optimization Strategy[b,c] for Each of the Systems[d] I to IV Treated in Either Cartesian (C) or Mixed (M) Coordinates

combination	I–C	I–M	II–C	II–M	III–C	III–M	IV–C	IV–M
NEB	127		77	97	87	37	52	82
S-MUL	77	47	117	77	87	52	77	52
S-CG	352*		347*	82	87	37	62	87
SS-MUL	100*	94*	70	82	68	17	82	29
SS-CG	133	124	31	183	43	21		83
CIS-MUL	117	87	102	67	57	52	67	62
CIS-CG	97	207	87	82	87	37	47	87

[a]Nudged elastic band, NEB; string, S; searching string, SS; climbing-image string, CIS. [b]Path optimization with conjugate-gradient (CG) or multiopt (MUL) procedures; see text. Calculations that did not converge within 35 iterations of the optimizer are marked by an asterisk. [c]Combinations of acronyms identify a path searching strategy, e.g., SS-CG refers to a searching-string method combined with a conjugate-gradient optimization procedure. [d]Omissions indicate instances where no valid path was delivered.

Of the two optimizers, multiopt and conjugate gradient, the former wins with $\langle \Delta n/\bar{n}_s \rangle = -0.15$ over the latter with $\langle \Delta n/\bar{n}_s \rangle = 0.12$ (Figure 2). For the 22 valid pairs available for comparison, the multiopt approach required fewer gradient calls in 13 cases, while the conjugate-gradient strategy was more efficient in only eight cases. A major factor for the difference is the fact that the conjugate-gradient method requires two gradient calls per iteration, as opposed to only one such call in the Hessian-based multiopt approach.

Among the chain-of-state methods, the searching string method is the most efficient one, requiring 17% fewer gradient calls than the average; the CI-string method as the next best method requires on average −5% (Figure 2). The searching string method failed once, for system IV, while the CI-string method never failed. The standard string method performs less well (Figure 2); two calculations did not converge within the allowed 35 iterations. The searching string method, demanding fewer gradient calls per iteration than the other approaches, also did not meet the convergence criterion of 35 iterations in two cases.

The ranking changes if one considers the number of chains to be built as a primary metric (Figure 2). This criterion correlates with the real time when the gradient calls are executed in parallel. We computed the average relative differences $\langle \Delta i/\bar{i}_s \rangle$ of states of a chain in analogous fashion to the measure $\langle \Delta n/\bar{n}_s \rangle$. With $\langle \Delta i/\bar{i}_s \rangle = 0.33$, the searching string method is the worst according to this new criterion, while the standard string method with as many failed convergences as the searching string method features $\langle \Delta i/\bar{i}_s \rangle = 0.01$. The CI-string method is the best according to this criterion, with $\langle \Delta i/\bar{i}_s \rangle = -0.26$ (Figure 2). The number of chains used in these procedures can be found in Table S5 of the Supporting Information.

A discrete path that fulfills common convergence criteria will not provide an estimate of the transition state with the accuracy desired in typical applications.[20,25] Even the CI-string method, for all optimizers and coordinate systems, does not accurately reproduce the reference geometry and energy of the transition state; as an example, see the path projections and energy profiles for system II, Figure 3. The deviation of the CI results from the reference transition structure is comparable to or larger than the differences across the variants of the CI-string method; in Cartesian coordinates, the maximum difference from the reference is ∼0.9 Å (!). The maximum energy difference of the climbing images to the reference transition state is ∼28 kJ/mol. Except for system III, all calculations ended with similar geometry and energy differences, see section S1 of the Supporting Information. Thus, we consider a TS estimate obtained from any chain-of-states methods only as starting point for a subsequent refinement by a dimer method.

In some cases, the searching-string and standard string methods yielded irregularities as indicated by several maxima in the energy profile. For this type of surface reaction, hydrogen atoms often move to a nearby local minimum before approaching the actual reaction site. In these and similar cases, we started the refinement by choosing that approximate transition structure which lies closest to the straight connection of initial and final states.

4.2. Evaluation of the Refinement Step. We compared the performance of the two dimer refinement methods, standard dimer and mDL, by applying them, as an example, to the 15 successful TS estimates obtained for the four systems I–IV from the standard string method (Table 3). We restricted

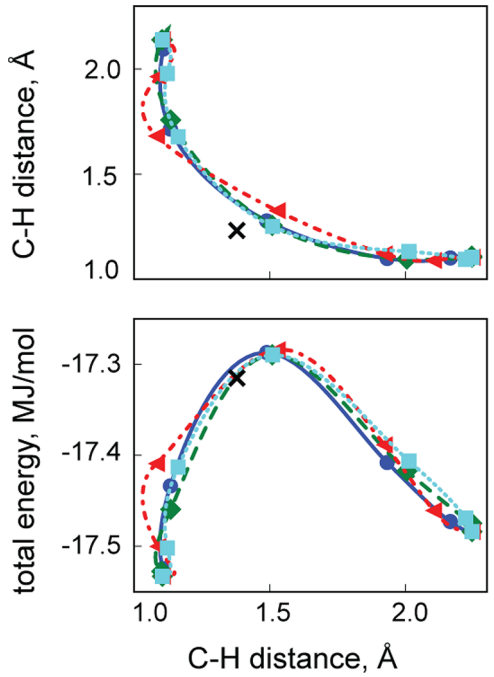

Figure 3. Reaction pathways (upper panel) and energy profiles (lower panel) for system II as determined by the CI-string method: all four pathways, obtained with Cartesian and mixed coordinates in combinations with the multiopt or conjugate-gradient optimizer. Crosses indicate the values of the reference transition state; positions of images on the interpolated paths are also marked. Circles, CG-CART; diamonds, MUL-CART; triangles pointing left, CG-MIX; triangles pointing right, MUL-MIX. For abbreviations, see Table 2.

the evaluation to this string method as all TS estimates generated by any of the string methods showed geometry and energy differences of similar size relative to the reference TS; see section S1 of the Supporting Information.

Three cases of the 15 starting geometries, all of them for system II, were found to converge to unexpected structures. Two unexpected structures resulted, one corresponding to a stationary point of higher order (with two negative eigenvalues), the other one a TS of a different process. For the two starting geometries generated by the conjugate-gradient optimizer, either the standard dimer or the mDL variant converged to one of the two unexpected structures. For the starting geometry in Cartesian coordinates, generated with the multiopt optimizer, both refinement methods converged to the stationary point of higher order. Although in this case, the result was not the desired one, these results are still useful for comparing the performance of the two implementations of the dimer method as they approach the same final results.

Disregarding those cases where the two refinement approaches did not converge to the same stationary point, there are 13 TS calculations to be compared. In nine cases, the mDL method required fewer gradient calls than the standard dimer approach. Averaged over these 13 calculations, the standard dimer method required 39 translation iterations and 191 gradient calls, while the mDL method needed 35 translation iterations and 150 gradient calls, Table 4. Variations in the number of gradient calls are mainly related to the fact that the mDL method requires only one gradient call per translation step (section 2.2) in contrast to two such gradient evaluations per translation step in the standard dimer approach.

dx.doi.org/10.1021/ct300728a | J. Chem. Theory Comput. XXXX, XXX, XXX−XXX

Table 4. Average Number of Gradient Calls Required for Dimer Refinements of Starting Geometries from the Standard String Method for Systems I to IV[a]

method	translation	rotation	total
standard dimer	77	114	191
modified dimer-Lanczos	35	115	150

[a]Averaging carried out over the 13 calculations that converged to the same structure for both refinement methods. Standard dimer and modified dimer-Lanczos methods required on average 39 and 35 iterations, respectively. Averages for the translation and rotation steps are also shown.

The number of gradient calls for mode rotations is comparable, Table 4.

Figure 4 shows the fluctuations in the total number of gradient calls as a function of the iteration index on the example

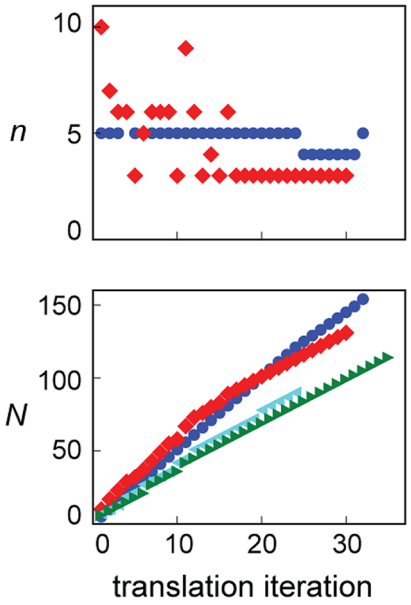

Figure 4. Number of gradient calls n (upper panel) and cumulative count N (lower panel) as a function of the iteration index for the dimer (blue circles) and modified dimer-Lanczos (red diamonds) methods on the example of one of the starting geometries of system III. By relaxing the mode convergence threshold from 0.01° to 0.02° (cyan triangles, pointing downward) and 0.03° (green triangles, pointing upward), the initial gradient call rate of the modified dimer-Lanczos method can be reduced (lower panel).

of one of the starting geometries. At the beginning of the optimization process, updating the mode consumes up to 10 gradient calls, the maximum allowed. Toward the end of the process, three gradient calls per iteration are needed with the mDL method, improving slightly upon the standard dimer method.

A significant fraction of gradient calls is spent for mode rotation, Table 4; there seems to be room for improvements. For one of the starting geometries, we carried out two additional calculations with relaxed requirements for mode vector convergence, Figure 4 (lower panel). By increasing the lower threshold of the rotation angle from 0.01° to 0.02° or 0.03°, the average number of gradient calls per step, required for mode rotations with the mDL method, dropped notably, from 3.4 to 2.8 and 2.3, respectively. The reduced accuracy in the mode vector might result in a larger number of translations; we observed 30, 24, and 35 iterations for the three successively larger threshold values, respectively. Yet, both calculations with a relaxed mode convergence criterion took fewer gradient calls, reducing the overall count from 132 to 91 and 115, respectively.

Considering only cases that properly converged, the results of the dimer methods exhibited maximum deviations from the reference TS of 0.06, 0.003, 0.05, and 0.11 Å in the Cartesian norm and 0.09, 0.33, 0.08, and 0.05 kJ/mol in energies, for systems I to IV, respectively. For the mDL method, the Cartesian norm yielded differences of 0.04, 0.02, 0.04, and 0.43 Å, and the energy differences were 0.04, 0.28, 0.06, and 1.15 kJ/mol, respectively.

4.3. Overall Performance of Method Combinations. Finally, to quantify the overall performance of the two-step TS search procedures provided by various method combinations, we refined the TS estimate of every path searching procedure, section 4.1, with the newly developed mDL method, the better one of the two dimer methods (section 4). Table 5 collects the

Table 5. Total Number of Gradient Calls When Applying Various Two-Step Procedures,[a] Path Optimization Followed by Refinement with the mDL Method, to Systems I to IV

comb.	I–C	I–M	II–C	II–M	III–C	III–M	IV–C	IV–M
NEB	319		262	225	240	163	249	271
S-MUL	284	202	*ho*	214	236	166	286	217
S-CG	479		536	*u*	235	169	268	237
SS-MUL	314	287	269	255	159	145	*u*	247
SS-CG	*u*	279	237	292	186	139		284
CIS-MUL	283	214	289	220	*u*	152	335	237
CIS-CG	274	375	283	*u*	*u*	168	327	227

[a]For the designations of the various methods, see Table 3. Omissions represent cases where path optimization failed. "*ho*" marks the case where a higher-order stationary point was located. "*u*" designates cases where the refinement did not converge to the intended transition state.

total number of gradient calls for these two-step procedures, path optimization plus mDL refinement. All refinement calculations converged, sometimes to an unexpected stationary point, section 4.2. Such unexpected results together with failed path optimizations make up the omissions in Table 5 and are not included in the following evaluations.

The average number of gradient calls, 167, for the mDL refinement step is approximately twice as large as the average number of gradient calls, 88, required in the preceding path optimization step. Obviously, for our convergence criteria, the choice of the refinement method is more important with respect to the number of gradient calls than the choice of the estimation step. This relation will change when one notably increases the number of chain images. Figure 5 shows category averages of the relative differences of the numbers of gradient calls from the pertinent system-specific averages, combining path estimate and refinement steps.

A combined TS search strategy appears to profit from the use of mixed coordinates. The resulting number of gradient calls is ∼10% lower than the overall average, or ∼20% lower on average than in the case of Cartesian coordinates, Figure 5. Due to the strong weight of the mDL refinement step in the combined statistics, the overall advantage of using the multiopt strategy for path optimization over the conjugate-gradient approach shrinks to ∼13% of the number of gradient calls, on average (Figures 2 and 5). Among the chain-of-state methods

dx.doi.org/10.1021/ct300728a | J. Chem. Theory Comput. XXXX, XXX, XXX–XXX

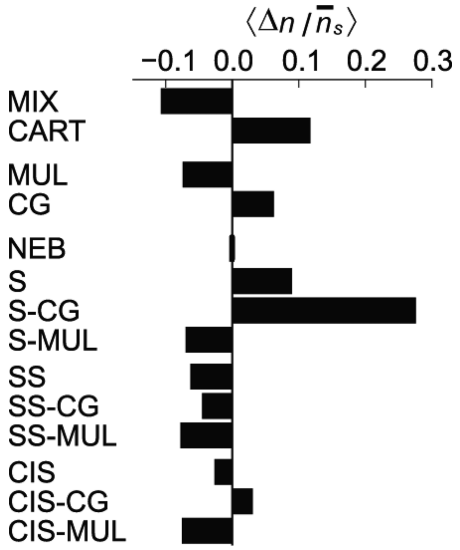

Figure 5. Category averages of the relative differences $\langle \Delta n/\bar{n}_s \rangle$ where $\Delta n = n - /\bar{n}_s$ is the difference of the number n of gradient evaluations for systems s = I–IV and the corresponding average $\bar{n}_s$, as required for the two-step transition state search, path optimization plus modified dimer-Lanczos refinement. Lower is better. Comparison of mixed (MIX) and Cartesian (CART) coordinates, of the two optimization methods, multiopt (MUL) and conjugate gradient (CG). Comparison of four chain-of-state methods: NEB, standard string (S), searching string (SS), and CI-string (CIS). For each of the string methods, three average values are shown: all optimizations as well as separate optimizations carried out with the path optimizers conjugate-gradient or multiopt.

the searching-string method is ahead by ∼6% fewer gradient calls compared to the average over all methods. The CI-string method is almost as efficient; it needs only ∼3% more evaluations (Figure 5). The efficiency of the chain-of-state methods is strongly affected by the optimizers applied. For the standard string method, the effect is particularly visible in Figure 5. When combined with the multiopt strategy, the standard string method exhibits an efficiency comparable to that of the searching string and CI-string methods. The searching string method is only slightly better when combined with the multiopt strategy than with the conjugate gradient method. Thus, the CI-string method is competitive with the searching string approach when either one is combined with the multiopt optimizer; both combinations are ∼7% better than the average over all methods.

The properties of the resulting TS approximations varied only moderately. TS energies of systems I to III scattered by 0.02–0.04 kJ/mol, as measured by the standard deviation. The Cartesian coordinates of the moving atoms showed a maximum absolute deviation of 0.04–0.09 Å as measured in the Cartesian norm. TS structures of system IV deviated more from the average: 0.47 kJ/mol for energies and 0.6 Å as maximum differences in atomic positions. This latter system also showed the largest standard deviation in the imaginary frequency, 7.2 cm^{-1}, from the reference data while system I showed the second largest standard deviation, 3.9 cm^{-1}. Detailed information on the deviations of energy and geometries related to the reference data are provided in section S2 of the Supporting Information.

4.4. Strategies in Case of Incorrect Transition States. Finally, we shall address the failures of the combined TS search strategy, as indicated by the 10 cases marked in Table 5. In these cases, the search yielded stationary points different from the desired transition states. In six cases, marked by "*u*" in Table 5, the refinement was only successful after the reaction path was improved by applying tighter convergence criteria. For a stationary point of second order, located with the mDL method ("*ho*" in Table 5), a single step of fixed length was carried out along the eigenmode with the least negative Hessian eigenvalue. In all these cases, a subsequent search with the mDL method converged to the correct transition state. This type of failure illustrates shortcomings of local transition state search strategies and underlines the importance of the path searching techniques and the use of a two-step approach.

Figure 6 illustrates this kind of failure for system II by showing the difference of two successive iterations of the path

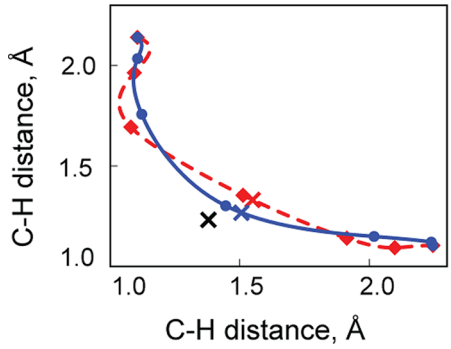

Figure 6. Projections of two approximations of the reaction path of the hydrogen shift reaction (system II), with standard convergence criteria Δg = 0.26 (dashed line) and its subsequent refinement with tighter convergence with Δg = 0.10 (solid line). The modified dimer-Lanczos method locates different transition states when started from the TS estimates of these two paths. Crosses on the pathways indicate the TS estimates; the reference TS is marked as a cross, off any of the pathways.

approximations projected onto the two C–H distances that change significantly during the reaction. The conjugate gradient optimization stopped because it reached the step convergence criteria with a gradient convergence of Δg = 0.26. The calculation was continued to Δg = 0.10. As a result, the subsequently applied mDL method converged toward the correct reference structure. This example demonstrates how small changes in the starting path may decide the success or failure of a two-step process.

In the remaining three cases, indicated as omissions in Table 5, already the path optimization failed to provide a reasonable estimate of the TS; see Table 3 and section 4.1. Using a different path optimization method is advisible in such cases.

For the six cases marked by "*u*" and the one case marked by "*ho*", the required numbers of gradient calls are provided in Table S6 of the Supporting Information.

4.5. Tests on Additional Systems. We used the four reactions V to VIII to verify the best combinations of methods as deduced from the study of systems I to IV. For these additional reactions, one of the favored string methods, searching string or CI-string, was combined with the superior optimizer (multiopt), followed by a mDL refinement. The calculations were carried out in mixed coordinates as they had been found to require fewer gradient calls, section 4.3.

4.5.1. Systems V and VI. For system V, the CI-string method required 17 iterations, amounting to 87 gradient calls, while the subsequent refinement with the mDL method needed 73

dx.doi.org/10.1021/ct300728a | J. Chem. Theory Comput. XXXX, XXX, XXX–XXX

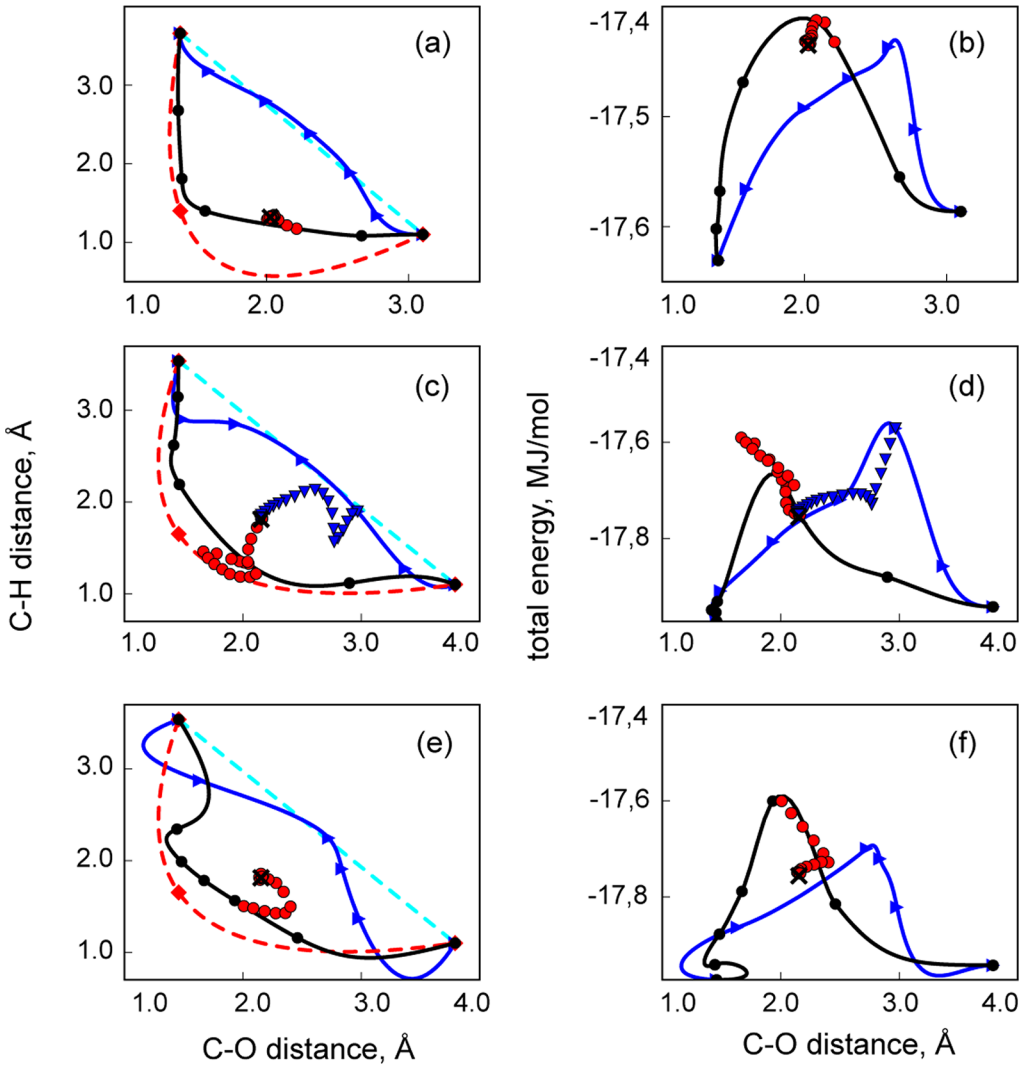

Figure 7. Path projections (left-hand column) and energy profiles (right-hand column) of the S_N2 reactions VII (CI-string method: a, b) and VIII (CI-string method: c, d; searching-string method: e, f), using the distances C−O and C−H. The starting path from a linear interpolation (cyan, dashed line) and the resulting converged path (blue, solid line with triangles) are to be compared with a parabolic interpolation (red, dashed line with diamonds) and the corresponding converged S_N2 reaction path (black, solid line with dots). The subsequent refinement (red dots or blue triangles) starts from the image of this path with the highest energy and is only shown when the optimization converged to the transition state of the S_N2 reaction.

gradient calls in addition, resulting altogether in 160 gradient calls for this two-step strategy. Path search with the searching string method (45 calls) plus mDL refinement (84 calls) required only 129 gradient calls. Note, however, that the path obtained by the searching string method exhibited a loop in the region of one of the minima, whereas the path obtained by the CI-string method did not.

With 99 degrees of freedom, system VI is the largest in our test set. The CI-string method for path optimization and mDL for refinement together amounted to 193 gradient calls. The strategy using the searching string method for path optimization required 227 gradient calls. In this case, the searching string method did not provide a converged path after 35 iterations, the final measure of gradient convergence being $\Delta g = 0.6$. For comparison, we note that the CI-image string method converged in 10 iterations. Yet, the two TS estimates were of similar quality. Refinement of the searching string estimate required 157 gradient calls, only few more than the refinement of the CI-string estimate with 141 gradient calls. The number of gradient calls spent for system VI is comparable to that of smaller systems, despite the much larger number of degrees of freedom. Both systems nicely corroborate that the CI-string and searching string methods, refined with the mDL method, are a sound choice for a two-step strategy, able to locate a TS at reasonable computational expense, as already concluded for systems I−IV.

4.5.2. Systems VII and VIII: The S_N2 Reactions. The reactions of systems VII and VIII are more complex than the preceding test cases as they are assumed to involve S_N2 reactions where hydrogen addition synchronously releases a hydroxyl group. For system VIII, the complexity is increased even more by the fact that methane is only very weakly bound to the surface. In these cases, a starting path, interpolated in linear fashion using mixed coordinates, might not be the best choice. The converged path does not differ much from this initial linear approximation. Especially the two relevant interatomic distances of the resulting TS estimate (C−H > 1.6 Å, C−O > 2.6 Å) beg the question whether these TS

dx.doi.org/10.1021/ct300728a | J. Chem. Theory Comput. XXXX, XXX, XXX−XXX

Table 6. Number of Gradient Evaluations Used for Various Two-Step Approaches, Combining a Path Searching Step (1) and a Refinement of the TS Approximation with the Modified Dimer-Lanczos Method (2), Applied to Systems I to VIII[a]

system		I	II	III	IV	V	VI	VIIa	VIIb	VIIIa	VIIIb
SS	1	94	82	17	29	45	70	27		94	59
	2	193	173	122	218	84	157				181
	total	287	255	139	247	129	227				240
CIS	1	87	67	52	62	87	52	42	97	62	142
	2	127	153	100	175	73	141		207	286	278
	total	214	220	152	237	160	193		304	420	420

[a]For the path search, the two best strategies, searching-string (SS) and climbing-image string (CIS), in mixed coordinates, were combined with the multiopt optimization (MIX-MUL). For systems VII and VIII, two sets of results are given, for initial pathways from (a) linear and (b) parabolic interpolation (see Figure 7). Omissions represent cases where the path search (step 1) failed or the refinement (step 2) converged to an undesired transition state or failed at all. For designations, see Table 2.

structures do correspond to an S_N1 reaction where first the OH group is abstracted by breaking the C−O bond, before the C−H bond is formed. For system VII, both methods, CI-string and searching string, were shown to converge eventually to a reaction path of S_N1 type.

Although the S_N1 reaction might be the one that the system would take in reality, it is desirable to examine how the methods examined are able to handle the more complex S_N2 variant. Therefore, we went beyond the linear interpolation of the initial guess of the S_N2 reaction path by adding an intermediate image and in this way constructed an initial path by parabolic interpolation.

For system VII the intermediate image was derived from the geometry of the reactant. The attacking hydrogen was placed in such a way that C−H = 1.4 Å and Pt−H = 1.7 Å; the C−O distance was kept as in the reactant's geometry, at 1.39 Å. Figure 7a compares linear and parabolic interpolations and the corresponding converged reaction paths as obtained by the CI-string method. Table 6 collects the number of gradient calls for the optimization of the parabolic starting path. The CI-string method used 97 gradient calls to convergence and the refinement to the S_N2 TS structure, 207 gradient calls, in total 304 gradient evaluations for this two-step procedure. The searching-string method produces a path far from the expected one, as a water molecule was formed when the TS search was started with the parabolic interpolation.

For system VIII, the refinement after the CI-string method, started with the linear interpolation, converged to the correct TS. Still, for comparison, we also examined a path search that started with a parabolic interpolation. The required third structure was constructed by rotating the methyl group and moving the adsorbed hydrogen from the platinum host toward the carbon center. Pertinent distances of the starting geometry were C−H = 1.65 Å, Pt−H = 1.89 Å, and C−O = 1.46 Å (Figures 7c,e). The CI-string method converged after 142 gradient calls to a path where hydrogen first moves to a bridge site on the surface before reacting with CH_3OH (not recognizable in the projection of Figure 7c). The resulting TS estimate was refined to the correct TS, requiring 278 additional gradient calls (Table 6). The searching-string method converged after only 59 gradient calls to a smooth S_N2 reaction path. The corresponding TS estimate was refined after 181 gradient calls to the correct TS (Figure 7e). Both initial pathways, starting from the linear or the parabolic interpolation, yielded TS estimates which were equally far away from the correct TS, with the maximum component of the displacement vector as large as 1.8 Å and 1.3 Å, respectively (Figures 7c,e). These deviations are among the largest calculated for all systems in this study when starting from reasonable initial guesses. None of the pathways describes the reaction well, resulting in many gradient calls during the mDL refinement. Still, local optimizations were able to locate eventually the correct TSs from either path approximation.

The resulting energy profiles of the two systems show one maximum each (Figures 7b,d,f), albeit at two different lengths of the C−O bond. We attribute the four approximate TS structures with C−O distances, which are notably longer than an activated bond, to the simultaneous formation of C−H bonds. The three converged pathways, derived from the initial parabolic interpolation, exhibit C−O distances of ∼2 Å, which are still in the range of activated bond lengths.

Pathways starting from the parabolic interpolation were more difficult to converge than the corresponding pathways starting with linear interpolation. This made systems VII and VIII more demanding, whereas system V and the large system VI had requirements comparable to the simpler systems I to IV.

5. CONCLUSIONS

We systematically evaluated various approaches for locating transition states (TSs) of reactions on metal surfaces. We employed a two-step strategy where a reaction path search for obtaining an estimate of a TS is followed by a refinement with a dimer method. We considered several methods for determining an approximate reaction path: standard string, nudged elastic band, climbing-image string (CI-string), and searching string. We examined two path optimizers, the well-established conjugate gradient method as a reference and a new steepest-descent image optimizer,[14] in combination with two types of coordinates. For estimating the TS, we used the CI method or a cubic spline extrapolation. For TS refinement, we evaluated two variations of the dimer method, the standard dimer method as well as a newly developed modified dimer-Lanczos (mDL) method. This latter new method features an alternative update of the mode vector and combines dimer information with a quasi-Newton approach. The mDL method reduced the number of gradient calls by about 20% on average. The number of gradient calls may be reduced even further by tuning the eigenmode convergence criteria. The TS refinement required about twice as many gradient calls as the method for obtaining a useful path approximation.

We chose a test suite of catalytic reactions on metal surfaces. For our systematic study, we used four systems with 14 to 15 moving atoms, including nine atoms of the uppermost layer of the substrate surface. Mixed Z-matrix/Cartesian coordinates outperformed plain Cartesian ones. The searching-string and the CI-string methods with a steepest-decent based optimizer

dx.doi.org/10.1021/ct300728a | J. Chem. Theory Comput. XXXX, XXX, XXX−XXX

were the most efficient approaches for obtaining an approximate path. The searching-string method has an advantage when one considers the average number of gradient calls (or CPU usage). On parallel architectures, the CI-string method may be preferable when the number of iterations in the optimization, or real time, is the measure.

Four additional test systems confirmed the preceding findings for the two best two-step methods. In particular, even for a system with 99 degrees of freedom, the number of gradient calls did not significantly grow. For S_N2 reactions, a three-point parabolic interpolation of an initial path notably improved chances for locating the correct TS.

In most cases where the dimer method converged to an unexpected structure, correct solutions were found by resuming path optimization with tighter convergence criteria and by producing a better starting point for the dimer refinement. With that refinement strategy, all CI-string calculations followed by an mDL refinement located the correct structure. One of the searching-string calculations failed due to a path with dissociating molecules. Thus, for the present set of eight example reactions on metal surfaces, the two-step strategy combining of the CI-string method for path optimization with mDL refinement turned out to be the best.

■ ASSOCIATED CONTENT

Supporting Information

Deviations of transition state estimates of the path searching and the refinement steps from the reference transition states of systems I to IV; number of chains for the path searching step; gradient call requirements for the failed optimization cases; Z-matrix connectivities for all adsorbates; geometries of all reactants, reference transition states, and products. This material is available free of charge via the Internet at http://pubs.acs.org.

■ AUTHOR INFORMATION

Corresponding Author

*E-mail: roesch@mytum.de.

Notes

The authors declare no competing financial interest.

■ ACKNOWLEDGMENTS

We thank Cheng-Chau Chiu, Duygu Basaran, and Zhi-Jian Zhao for their help with setting up the test systems. We are grateful to Sven Krüger for numerous discussions. A.N. acknowledges the hospitality of the colleagues at the Quantum Chemistry Laboratory of the Institute of Chemistry and Chemical Technology in Krasnoyarsk, Russian Federation, as well as generous support of the Munich Centre of Advanced Computing and the International Graduate School of Science and Engineering, both at Technische Universität München. The work of N.R. is supported by Fonds der Chemischen Industrie (Germany). We also acknowledge generous computing resources at Leibniz Rechenzentrum München.

■ REFERENCES

(1) Schlegel, H. B. *J. Comput. Chem.* **2003**, *24*, 1514−1527.
(2) Henkelman, G.; Jóhannesson, G.; Jónsson, H. Methods for Finding Saddle Points and Minimum Energy Paths. In *Progress on Theoretical Chemistry and Physics*; Schwartz, S. D., Eds.; Kluwar Academic Publishers: Dordrecht, The Netherlands, 2000; pp 269−300.
(3) Hratchian, H. P.; Schlegel, H. B. Finding minima, transition states, and following reaction pathways on ab initio potential energy surfaces. In *Theory and Applications of Computational Chemistry: The First Forty Years*, 1st ed.; Dykstra, C. E., Frenking, G., Kim, K. S., Scuseria, G. E., Eds.; Elsevier: Amsterdam, The Netherlands, 2005; pp 195−251.
(4) Schlegel, H. B. *Wiley Interdiscip. Rev.: Comput. Mol. Sci.* **2011**, *1*, 790−809.
(5) Shang, C.; Liu, Z.-P. *J. Chem. Theory Comput.* **2010**, *6*, 1136−1144.
(6) Wang, H.-F.; Liu, Z.-P. *J. Am. Chem. Soc.* **2008**, *130*, 10996−11004.
(7) Jónsson, H.; Mills, G.; Jacobsen, K. W. In *Classical and Quantum Dynamics in Condensed Phase Simulations*; Berne, B. J.; Ciccotti, G.; Coker, D. F., Eds.; World Scientific: Lerici, Italy, 1997; pp 385−404.
(8) Henkelman, G.; Jónsson, H. *J. Chem. Phys.* **2000**, *113*, 9978−9985.
(9) Chen, M.; Cai, Z.-Z.; Yang, X.-B.; Zhu, M.; Zhao, Y.-J. *Surf. Sci.* **2012**, *606*, L45−L49.
(10) Moras, G.; Pastewka, L.; Walter, M.; Schnagl, J.; Gumbsch, P.; Moseler, M. *J. Phys. Chem. C* **2011**, *115*, 24653−24661.
(11) Martínez de la Hoz, J. M.; Balbuena, P. B. *J. Phys. Chem. C* **2011**, *115*, 21342−21333.
(12) Weinan, E.; Ren, W.; Vanden-Eijnden, E. *Phys. Rev. B: Condens. Matter Mater. Phys.* **2002**, *66*, 052301.
(13) Burger, S. K.; Yang, W. *J. Chem. Phys.* **2006**, *124*, 054109.
(14) Chaffey-Millar, H.; Nikodem, A.; Matveev, A. V.; Krüger, S.; Rösch, N. *J. Chem. Theory Comput.* **2012**, *8*, 777−786.
(15) Quapp, W. *J. Chem. Phys.* **2005**, *122*, 174106.
(16) Peters, B.; Heyden, A.; Bell, A. T.; Chakraborty, A. *J. Chem. Phys.* **2004**, *120*, 7877−7886.
(17) Goodrow, A.; Bell, A. T.; Head-Gordon, M. *J. Chem. Phys.* **2009**, *130*, 244108.
(18) Goodrow, A.; Bell, A. T.; Head-Gordon, M. *J. Chem. Phys.* **2008**, *129*, 174109.
(19) Behn, A.; Zimmerman, P. M.; Bell, A. T.; Head-Gordon, M. *J. Chem. Phys.* **2011**, *135*, 224108.
(20) Kanai, Y.; Takeuchi, N.; Car, R.; Selloni, A. *J. Phys. Chem. B* **2005**, *109*, 18889−18894.
(21) Henkelman, G.; Uberuaga, B. P.; Jónsson, H. *J. Chem. Phys.* **2000**, *113*, 9901−9904.
(22) Weinan, E.; Ren, W.; Vanden-Eijnden, E. *J. Chem. Phys.* **2007**, *126*, 164103.
(23) Ozbek, M. O.; Onal, I.; van Santen, R. A. *J. Catal.* **2011**, *284*, 230−235.
(24) Jackson, B.; Nave, S. *J. Chem. Phys.* **2011**, *135*, 114701.
(25) Chin, Y.-H.; Buda, C.; Neurock, M.; Iglesia, E. *J. Am. Chem. Soc.* **2011**, *133*, 15958−15978.
(26) Zhao, P.; Su, Y.; Zhang, Y.; Li, S.-J.; Chen, G. *Chem. Phys. Lett.* **2011**, *515*, 159−162.
(27) Ozbek, M. O.; Onal, I.; van Santen, R. A. *J. Phys.: Condens. Matter* **2011**, *23*, 404202.
(28) Yang, Z.; Zhang, Y.; Wang, J.; Ma, S. *Phys. Lett. A* **2011**, *375*, 3142−3148.
(29) Lin, S.; Xie, D.; Guo, H. *J. Mol. Catal. A: Chem.* **2012**, *356*, 165−170.
(30) Özbek, M. O.; Önal, I.; van Santen, R. A. *ChemCatChem* **2011**, *3*, 150−153.
(31) Peng, G.; Sibener, S. J.; Schatz, G. C.; Mavrikakis, M. *Surf. Sci.* **2012**, *606*, 1050−1055.
(32) Henkelman, G.; Jónsson, H. *J. Chem. Phys.* **1999**, *111*, 7010−7022.
(33) Heyden, A.; Bell, A. T.; Keil, F. J. *J. Chem. Phys.* **2005**, *123*, 224101.
(34) Kästner, J.; Sherwood, P. *J. Chem. Phys.* **2008**, *128*, 014106.
(35) Fajín, J. L. C.; Cordeiro, M. N. D. S.; Illas, F.; Gomes, J. R. B. *J. Catal.* **2009**, *268*, 131−141.
(36) Cao, X.-M.; Burch, R.; Hardacre, C.; Hu, P. *Catal. Today* **2011**, *165*, 71−79.

(37) Xu, L.; Xu, Y. *Catal. Today* **2011**, *165*, 96−105.
(38) Liu, B.; Greeley, J. *J. Phys. Chem. C* **2011**, *115*, 19702−19709.
(39) Basaran, D.; Genest, A.; Rösch, N. *J. Catal.* **2012**, *287*, 210−213.
(40) Moskaleva, L. V.; Aleksandrov, H. A.; Basaran, D.; Zhao, Z.-J.; Rösch, N. *J. Phys. Chem. C* **2009**, *113*, 15373−15379.
(41) Zhao, Z.-J.; Moskaleva, L. V.; Aleksandrov, H. A.; Basaran, D.; Rösch, N. *J. Phys. Chem. C* **2010**, *114*, 12190−12201.
(42) Zhao, Z.-J.; Moskaleva, L. V.; Rösch, N. *J. Catal.* **2012**, *285*, 124−133.
(43) Koslover, E. F.; Wales, D. J. *J. Chem. Phys.* **2007**, *127*, 134102.
(44) Olsen, R. A.; Kroes, G. J.; Henkelman, G.; Analdsson, A.; Jónsson, H. *J. Chem. Phys.* **2004**, *121*, 9777−9792.
(45) Sheppard, D.; Terrell, R.; Henkelman, G. *J. Chem. Phys.* **2008**, *128*, 134106.
(46) Klimeš, J.; Bowler, D. R.; Michaelides, A. *J. Phys.: Condens. Matter* **2010**, *22*, 074203.
(47) Nikodem, A.; Chaffey-Millar, H.; Matveev, A.; Rösch, N.; *ParaTools 2.0*; Technische Universität München: München, 2012.
(48) Nocedal, J.; Wright, S. J. *Numerical Optimization*, 2nd ed.; Springer Series in Operations Research and Financial Engineering, Springer: New York, 2006.
(49) Heyden, A.; Peters, B.; Bell, A. T.; Keil, F. J. *J. Phys. Chem. B* **2005**, *109*, 1857−1873.
(50) Bahn, S. R.; Jacobsen, K. W. *Comput. Sci. Eng.* **2002**, *4*, 56−66.
(51) Kresse, G.; Furthmüller, J. *Comput. Mater. Sci.* **1996**, *6*, 15−50.
(52) Kresse, G.; Hafner, J. *Phys. Rev. B: Condens. Matter Mater. Phys.* **1994**, *49*, 14251−14269.
(53) Perdew, J. P.; Wang, Y. *Phys. Rev. B: Condens. Matter Mater. Phys.* **1992**, *45*, 13244−13249.
(54) Kresse, G.; Joubert, D. *Phys. Rev. B: Condens. Matter Mater. Phys.* **1999**, *59*, 1758−1775.
(55) Blöchl, P. E. *Phys. Rev. B* **1994**, *50*, 17953−17979.
(56) Altmann, S. L. *Rotations, Quaternions and Double Groups*; Oxford University Press: New York, 1986.
(57) Alcalá, R. *J. Catal.* **2003**, *218*, 178−190.
(58) Jasper, A. W.; Klippenstein, S. J.; Harding, L. B.; Ruscic, B. *J. Phys. Chem. A* **2007**, *111*, 3932−3950.